Dynamic Properties of the Guanine Nucleotide Binding Protein α Subunit and Comparison of Its Guanosine Triphosphate Hydrolase Domain with That of *ras* p21[†]

Luciane V. Mello,*[,‡,§] Daan M. F. van Aalten,[‡,||] and John B. C. Findlay[‡]

School of Biochemistry and Molecular Biology, University of Leeds, Leeds LS2 9JT, U.K., and National Centre of Genetic Resources and Biotechnology−Cenargen/Embrapa, SAIN-Parque Rural, 70789-970 Brasilia, DF, Brazil

Received June 11, 1997; Revised Manuscript Received November 19, 1997

ABSTRACT: The dynamic properties of the α-subunit of bovine transducin ($G\alpha_t$) were studied using molecular dynamics simulations and essential dynamics analyses. The helical domain of transducin seems to move toward the guanosine triphosphate hydrolase (GTPase) domain. Our studies suggest that this movement is facilitated by a hinge bending motion that is centered on residues Gly56 and Gly179 and that this motion may be involved in GDP release and GTP hydrolysis. The dynamic properties of the GTPase domain of $G\alpha_t$-GDP were compared to those of *ras* p21 and reveal a significant degree of similarity, indicating common dynamic properties for an equivalent domain in two different proteins.

G-proteins[1] are the cytosolic messengers for the largest gene family in vertebrates, the G-protein-coupled receptors. G-proteins are involved in a wide variety of signal-transduction events controlling important processes such as cell division and differentiation (Barbacid, 1987; Gibbs et al., 1985; Kleus et al., 1994). External stimuli generate signals that are transduced to the cytosolic side of the membrane where heterotrimeric G-proteins interact with the transmembrane receptors, thereby initiating the GTPase cycle. Recently, the crystal structure of the visual heterotrimeric G-protein transducin (G_t) was determined (Lambright et al., 1996), revealing that the Gα subunit has three distinct structural components: the helical domain ($\alpha_A-\alpha_F$), the GTPase domain (a six-stranded β-sheet surrounded by six helices, $\alpha_1-\alpha_5$ and α_G), and an N-terminal helix (α_N). Between the two domains is a cleft, which is occupied by GDP and GTP in the inactive and active forms of the protein, respectively. In the GDP-bound form, Gα is associated with the $\beta\gamma$ complex and possibly with a receptor in the cell membrane. On G-protein activation, GDP−GTP exchange occurs and Gα dissociates from both the receptor and the $\beta\gamma$ complex. Gα-GTP and often also the $\beta\gamma$ complex then interact with the appropriate effector proteins. Finally, an intrinsic GTPase activity in the Gα subunit hydrolyzes bound GTP to GDP and the protein returns to the inactive GDP-bound state (Berstein et al., 1992; Noel et al., 1993). The crystal structures of bovine Gα complexed with GTP (Noel et al., 1993) and with GDP (Lambright et al., 1994) have been determined and have revealed that there are three regions (called switch I, II, and III) which undergo conformational change on ligand exchange.

There are three major families of proteins that possess GTPase activities and are structurally related: *ras* p21, the heterotrimeric G-proteins, and the elongation factors. Mammalian *ras* genes encode proteins of 189 residues with approximate molecular masses of 21 kDa, hence named the p21 proteins. They play an important role in the regulation of cell growth and differentiation and have been strongly implicated in the process of malignant cell transformation (Pincus et al., 1987). The crystal structure of the GDP-bound form of *ras* p21 was described by Tong et al. (1991). Here, we report the dynamics properties of Gα complexed with GDP, using computer simulation, and compare them with those for *ras* p21. This dynamic analysis reveals large concerted fluctuation of atoms, which might be of functional significance. Experiments involving mutational analysis could reveal whether this is indeed true.

EXPERIMENTAL PROCEDURES

Molecular Dynamics. The simulations were started from the $G\alpha_t$-GDP (Lambright et al., 1994) crystal structure. The molecular dynamics (MD) calculations were performed with GROMOS (van Gunsteren & Berendsen, 1987) using the force field that is specific for proteins in a water environment. The protons of the histidine residues were placed on the Nδ1 or Nϵ2 atoms as required by the local hydrogen-bonding patterns. The overall charge on the GDP molecule was −2

[†] This work was supported by the National Centre of Genetic Resources and Biotechnology-Cenargen/Embrapa, Brazil, and benefitted from the use of computer facilities at EMBL (European Union Access to Large Scale Facilities, Grant REBCHGECT940062).

* To whom correspondence should be addressed: fax ++ 44 113 2333167, tel ++ 44 113 2332987, E-mail bmblvm@bmb.leeds.ac.uk.

[‡] University of Leeds.

[§] National Centre of Genetic Resources and Biotechnology.

[||] Present address: Keck Structural Biology, Cold Spring Harbor Laboratory, 1 Bungtown Road, Cold Spring Harbor, NY 11724.

[1] Abbreviations: ED, essential dynamics; EM, energy minimization; $G\alpha_t$, G-protein transducin α-subunit; GAP, guanosine triphosphate hydrolase activating protein; GDP, guanosine diphosphate; G-protein, guanine nucleotide binding protein; G_i, G-protein that mediates the inhibition of adenylate cyclase; GTPase, guanosine triphosphate hydrolase; $G\alpha_t$-GDP, guanosine diphosphate-bound G-protein transducin α-subunit; MD, molecular dynamics; p21 *ras*, C−H− *ras* p21 oncogene protein; p21 *ras*-GDP, guanosine diphosphate-bound *ras*.

S0006-2960(97)01402-5 CCC: $15.00
Published on Web 02/13/1998

in pH 7.0. The distances between the magnesium ion and its ligands, side-chain hydroxyl groups of Ser43 and an oxygen of the β-phosphate of GDP, were restrained, using a force constant of 4500 kJ mol^{-1} nm^{-2}. For solvation, the protein was placed in a truncated octahedral box with sides of 84.91 Å. The remaining space was filled with water, resulting in the addition of 8579 water molecules.

First, a short energy minimization (EM) using a steepest descent algorithm was performed until no significant energy changes could be detected. The MD simulation was then carried out at a temperature of 300 K, a time step of 2.0 fs, a nonbonded cutoff radius of 8 Å, a long-range Coulomb cutoff radius of 10 Å, a temperature coupling constant of 0.1 ps, and a pressure coupling constant of 0.5 ps. After the MD simulation reached equilibrium, as assessed by evaluation of global geometrical properties (see below), it was continued for a further 500 ps. These resulting trajectories were employed in the essential dynamics (ED) analyses.

Analyses of secondary structure and hydrogen bonds of Gα_t-GDP during the MD simulations were performed using DSSP (Kabsch & Sander, 1983) and WHAT IF (Vriend, 1990) in order to check the quality of these simulations.

Essential Dynamics. Essential dynamics was previously described by Amadei et al. (1993) and is based on the diagonalization of the covariance matrix, built from atomic fluctuations relative to their average positions:

$$C_{ij} = \langle (X_i - X_{i,o})\,(X_j - X_{j,o}) \rangle$$

in which X_i and X_j are the separate x, y, z, coordinates of the C_α atoms, and X_o are the average positions of the coordinates and the average is calculated over all structures. A set of eigenvalues and eigenvectors is obtained by diagonalizing this matrix. The eigenvectors represent concerted motions of atoms in Cartesian space, and the eigenvalues give the amplitudes of the motions.

The position of each individual structure along an eigenvector may be investigated by projection:

$$d_{ij} = x_i \eta_j$$

where x_i is a structure, η_j is an eigenvector, and d_{ij} is the displacement of the ith structure along the jth eigenvector with respect to the average structure. This allows, for instance, the study of the time dependence of a certain motion during an MD simulation. The structure corresponding to such a projection can be studied as follows:

$$x_{ij} = x_0 + d_{ij}\eta_j$$

where x_0 is the average structure, d_{ij} is the projection described above, and η_j is an eigenvector.

A useful tool to compare two systems is combined essential dynamics (COMB) (van Aalten et al., 1995a). The trajectories from two simulations of similar systems (for instance, a wild-type protein and a mutant) are concatenated. This concatenated trajectory is then used for essential dynamics analysis. Analysis of the projection of the two separate trajectories on these "combined" eigenvectors can reveal similarities and differences in structure and dynamics between the systems being compared.

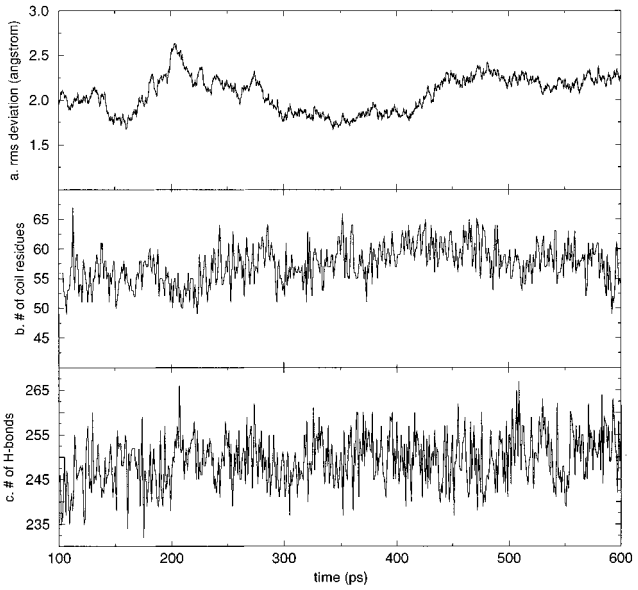

FIGURE 1: (a) Rms deviation of structure during the last 500 ps of the MD simulation in water compared with the crystal structure (Cα only). (b) Number of residues in random coil conformation. (c) Number of backbone−backbone hydrogen bonds in the MD simulation.

To quantify visually observed hinge bending motions described by an eigenvector, the two most conformationally distant structures found by projection of the trajectory on the eigenvectors were analyzed using the moving window RMS method (van Aalten et al., 1995b). In this approach, two configurations are superposed using a sliding window of 31 amino acids and the rms deviations of all Cα positions in each window are calculated. Peaks in the rms values versus the number of the residue in the middle of the window indicate hinge bending.

GTPase Domain Comparison. A tertiary structure alignment of the crystal structures of Gα_t-GDP and *ras*-GDP was performed using the WHAT IF superposition option (Vriend, 1990). The parts of the protein that were present in both structures were selected, forming a common core. This core consist of 84 residues, in which all α-helices or β-sheets present in either G-protein and *ras* were included. Therefore, it represents the overlapping regions of the Gα and *ras* GTPase domain ($\alpha_1-\alpha_5$ and $\beta_1-\beta_6$). These residues were extracted from the MD simulations of Gα_t-GDP described here and of *ras*-GDP described by Mello et al. (1997). The aim was to analyze the dynamics of the common GTPase domain. For this, an essential dynamics combined analysis was performed using 400 ps of each of these simulations.

RESULTS

Gα_t-GDP Analysis. The root-mean-square (rms) deviations between the positions of Cα atoms in the structures arising from the MD simulations and those in the Gα_t-GDP crystal structure are shown in Figure 1a. The number of residues in a coil conformation (Figure 1b) and the number of backbone−backbone hydrogen bonds (Figure 1c) computed during the Gα_t-GDP MD simulation in water show no significant drift. This indicates that the tertiary structure of Gα_t-GDP remains stable throughout the simulation and one can reliably interpret the observations.

The eigenvectors and eigenvalues were obtained by diagonalization of the covariance matrix constructed from

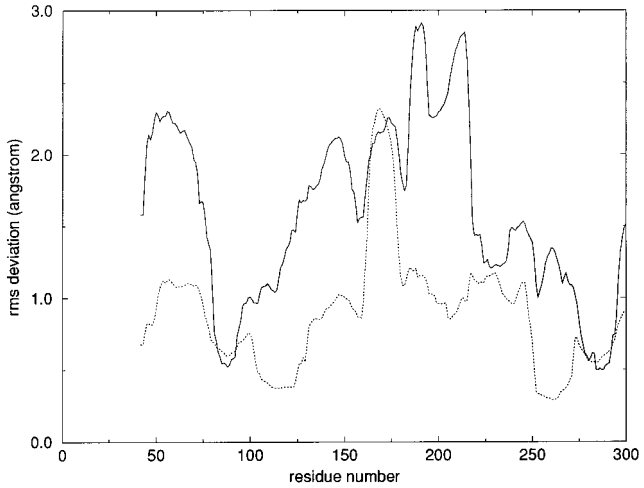

FIGURE 2: Output from the shifting-window rms method using frames from the $G\alpha_t$-GDP simulated in water, projected onto the first and second eigenvectors calculated from their covariance matrix. Solid line, eigenvector 1: dotted line, eigenvector 2.

the $G\alpha_t$-GDP simulation, as explained in the Experimental Procedures section. Only a few eigenvectors with relatively large eigenvalues were obtained, a feature observed before for most other proteins (Amadei et al., 1993; van Aalten et al., 1995b). About 71% of the motion in the sampled configurational space can be described by five eigenvectors with the largest eigenvalues.

We concentrate our analysis on the motion described by eigenvectors 1 and 2, which appears to be a rigid-body rotation between the two main (helical and GTPase) domains in the protein. Shifting-window rms calculations (Figure 2) employed to estimate positions of hinge residues suggest hinge bending motions around residues Gly 56, Gly 148, Gly 199, and Gly 213 for eigenvector 1 and around Gly 179 for eigenvector 2.

Gly 56 is part of the linker 1 region that connects the helical and GTPase domains. Gly199 and Gly213 are located in the loops before and after α-helix 2 (the switch II region), respectively. It is known that this latter region undergoes conformational change upon ligand exchange (Lambright et al., 1994). Gly 179 lies in the linker 2 region. It seems that glycines 56 and 179 are involved in the motion between the two domains in eigenvectors 1 and 2, respectively. A sequence alignment of Gα subunits shows that Gly 56 and Gly 179 are conserved in the family, suggesting an important role for these residues.

Table 1: Distances between Selected Residues of the Minimum and Maximum Projection Structures of Eigenvectors 1 and 2[a]

		distance (Å)	
		maximum proj.	minimum proj.
EV1	G92−G288	43.4	33.2
	A95−K276	35.8	26.9
	D127−E39	19.3	14.8
	D129−S271	28.9	21.6
	E131−V231	11.0	4.2
	A148−S43	17.0	15.9
EV2	V231−E39	14.3	11.3
	V231−G113	26.9	24.4
	V231−S173	23.6	19.4
	V231−S202	23.2	22.7

[a] See Figure 4. EV1 = eigenvector 1; EV2 = eigenvector 2.

The Cα−Cα distance difference matrixes for these eigenvectors (Figure 3) further confirm a motion between the helical and the GTPase domain in Gα subunits. As a further illustration of this motion, Table 1 shows the distances between selected residues involved in the movement described by eigenvectors 1 and 2. These residues are indicated in Figure 4, which shows the superpositions of the minimum and the maximum projections for both eigenvectors. These (minimum and maximum) projection structures correspond to the two extremes structures along an eigenvector during the simulation. The centers of mass of each domain for the minimum and maximum projections of both eigenvectors were measured. The distances between corresponding centers of mass were 27.6 and 28.8 Å for the maximum and minimum projections, respectively, of eigenvector 1 and 27.3 and 27.7 Å for the equivalent projections of eigenvector 2. Thus, in eigenvector 1, the helical and the GTPase domains move with respect to one another, opening and closing the cleft between them where the ligand binds (Figure 4a). In eigenvector 2, the helical domain shows less difference between the two extreme structures, but residues that surround the ligand binding cleft in the GTPase domain move toward each other (Figure 4b).

GTPase Domain Analysis: Gα vs ras p21. Sequence alignment of $G\alpha_t$ and *ras* p21 indicates an identity of 19.9%. Despite this low sequence conservation, their 3D structures reveal similar folds, which are nearly superimposable. The

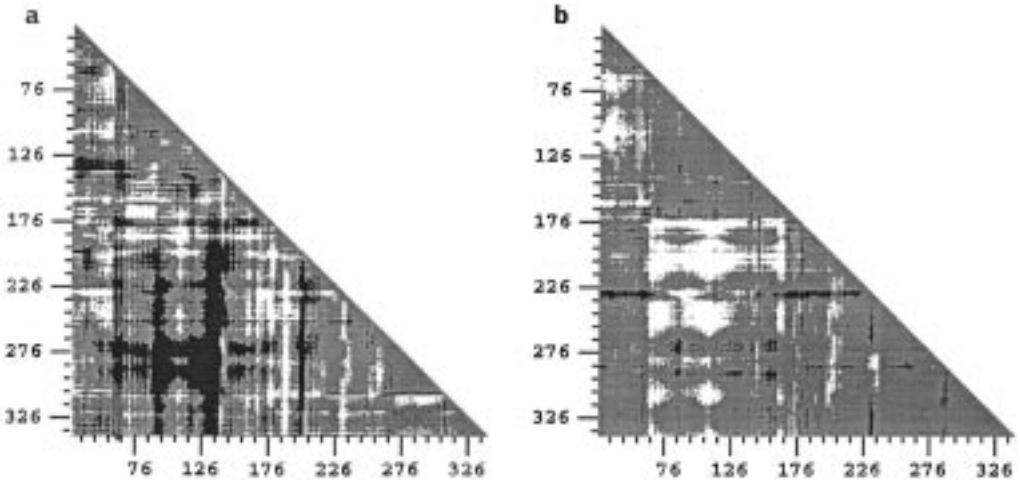

FIGURE 3: Cα−Cα distance matrix of eigenvectors 1 (a) and 2 (b) from 500 ps of the trajectories of $G\alpha_t$-GDP simulated in water.

FIGURE 4: Stereo pictures of the superposition of the minimum and the maximum projection structures of $G\alpha_t$ showing the kind of motion described by eigenvectors 1 (panel a) and 2 (b) (white and black coils, respectively). (a) Movement between the helical and the GTPase domains, opening and closing a pocket, exposing and protecting the ligand. (b) residues from the GTPase domain that surround the ligand pocket move closer and further apart, oscillating. * and + show the positions of Gly 56 and Gly 179; these are the most likely residues allowing this motion. The GDP molecule is shown in ball-and-stick form.

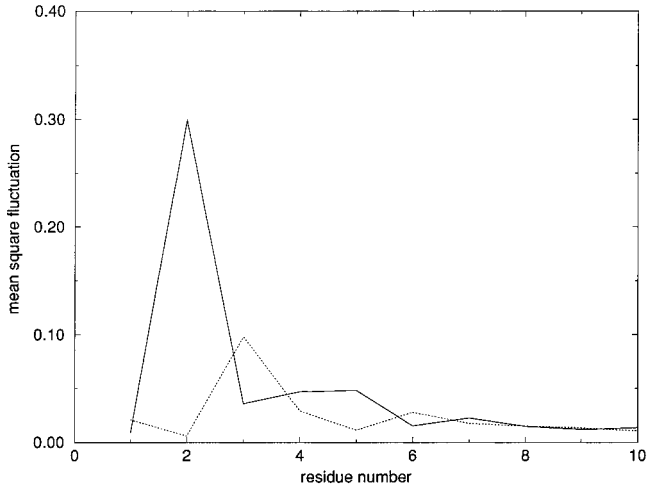

FIGURE 5: Mean square fluctuation of the projections of $G\alpha_t$-GDP (solid line) and *ras* p21-GDP (dotted line) trajectories projected onto the COMB eigenvector set.

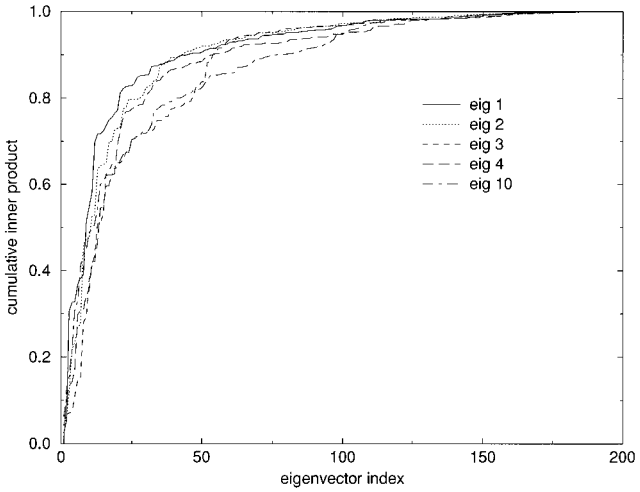

FIGURE 6: Cumulative square inner products between eigenvectors obtained from $G\alpha_t$-GTPase domain MD simulation and eigenvectors from *ras* p21 simulation.

major differences are the "insertion regions" present in $G\alpha_t$. The residues that have a functional role are highly conserved and are located at similar positions in the two proteins. For example, Thr177 and Gly199 in $G\alpha_t$ (corresponding to Thr35 and Gly60 in *ras* p21, respectively) are involved in binding the γ-phosphate of GTP and the Mg^{2+} ion.

Figure 5 shows the mean square fluctuation in the projections of the two trajectories onto the eigenvectors calculated from the COMB trajectory. The plot indicates that, except for the motion described by eigenvector 2, there are elements of similarity in patterns of motion of the GTPase domains of the two proteins. Figure 6 shows the projection of single eigenvectors 1−4 and 10 from the G protein simulation onto the eigenvector set from the *ras* simulation. It indicates that the former eigenvectors are represented by the first few eigenvectors from *ras*. In other words, even though eigenvector 2 suggests a difference in fluctuation between the two proteins, the overall motions in the GTPase core of both proteins are essentially the same. The motion described by eigenvector 2 is present in $G\alpha_t$ but constrained in *ras* p21. The residues involved here (Figure 7) mainly face the helical domain and move toward it. It may be that

FIGURE 7: Three-dimensional representation of $G\alpha_t$-GDP showing the main residues (thick line) involved in the motion described by eigenvector 2 from the COMB analyses between $G\alpha_t$ and *ras* p21 GTPase domain. The GDP molecule is shown in ball-and-stick form.

this kind of motion is related to the presence of the helical domain, which would explain its absence in the *ras* protein. Two of these regions (residues 34−43 and 186−190) are also present in eigenvector 1 from the $G\alpha_t$ single analysis, which describes the motion between the two domains.

DISCUSSION

Ligand-binding proteins have been analyzed in their unliganded and liganded forms, and it has been found that many assume a different conformation upon ligand binding. In many proteins, large conformational transitions involve the relative movement of almost rigid structural elements (Schulz, 1991; Marques & Sanejouand, 1995). It seems that such domain motions require hinge regions in the protein, more than a simple rotation of a main-chain dihedral angle. The importance of glycines in hinge bending regions has been discussed (van Aalten et al., 1997); glycines have an important role in the internal mobility of the proteins, which can be important for their functions. It seems that glycine residues in particular allow a substantial flexibility of protein regions in their vicinities due to their dihedral angle freedom, although other residues are also likely to be involved in hinge bending motions. Yeast phosphoglycerate kinase is formed from two domains and the cleft between them accommodates the substrates. Studies show that His388 is heavily involved in the domain motion, which was substantial affected when this residue was replaced by glutamic acid (Graham et al., 1991). Adenylate cyclase is similar in having a cleft formed by two domains. This enzyme binds to two different substrates (ATP and AMP), and a large conformational change is expected to facilitate protection of ATP from hydrolysis. An open form structure was observed when the protein was not complexed with either substrate, a half-closed form after binding AMP (Diederichs & Schulz, 1991), and a fully closed form after binding both substrates (Mueller & Schulz, 1988). The differences between the three forms were analyzed, revealing a large relative structural change of the two polypeptide domains (Schulz et al., 1990).

Essential dynamics analysis of $G\alpha_t$-GDP molecular dynamics simulations reveal a hinge bending motion between the helical and the GTPase domains, which appears to be dependent on conformational flexibility around residues Gly 56 and Gly 179. It is known that, after being activated by the receptor, $G\alpha$ has a lower affinity for GDP, which is released and replaced by GTP. In *ras* proteins, the nucleotide binding site is relatively freely accessible, while it is occluded in G-proteins due to the presence of the helical domain. Activated rhodopsin may open the nucleotide binding site cleft in transducin (Lambright et al., 1994). Thus, we believe that the motion between the two domains, revealed in this study, may be necessary for the processes that facilitate GDP release and GDP/GTP exchange.

Arg 174, absent in *ras* proteins, has been implicated as a key residue in GTP hydrolysis. It is located in the linker II region. The corresponding region of *ras* proteins, the "effector loop region" has been shown to bind GAPs. Ahmadian et al. (1997) showed that GAPs supply a catalytic residue, termed the "arginine finger", to the active site of *ras*, thereby increasing the GTP hydrolysis rate by over 1000-fold. Arg 174 is in a flexible region as revealed by the simulation of the GDP form, but it would be expected that this region is more restrained in the GTP form of the α subunit. The limitation of this motion may be important to keep catalytically important residues in their active positions. The importance of the helical domain for GTP hydrolysis has been the subject of some debate. Noel et al. (1993) suggested that the helical domain forms a barrier to ligand binding or dissociation and accounts for the slow rate of intrinsic nucleotide exchange. However, Markby et al. (1993), working with the helical and GTPase domains as separate fragments, showed an increase in GTP hydrolysis by the GTPase domain in the presence of the helical domain. They suggested that the helical domain can act biochemically as a GAP (GTPase activating protein). In this respect, it may resemble the RGS (regulator of G-protein signaling) family of proteins that has recently been described as GAP-like equivalents for $G\alpha$ subunits. It has been shown that RGS proteins stimulate the rate of GTP hydrolysis by different G-proteins (Watson et al., 1996; Hunt et al., 1996; Berman et al., 1996; and Koelle, 1997). Tesmer et al. (1997) demonstrated that $G\alpha_i$-AlF_4^+ contacts RGS4 via residues situated in the three switch regions and that the helical domain of $G\alpha_i$ makes no significant interactions with RGS4. They suggested that RGS proteins may increase the rate of GTP hydrolysis in G-proteins using a mechanism different to that adapted by GAP proteins with respect to *ras*. Muegge et al. (1996) showed that GAP proteins make a contact either with the γ-phospate group or with the $\beta\gamma$ bridging oxygen atom of the GTP molecule. Thus, GAP proteins have a direct involvement in the hydrolysis process, while RGS proteins operate as inhibitors of effector binding. It is known that heterotrimeric G-proteins have a higher intrinsic rate of GTP hydrolysis than *ras* p21. Therefore, if the helical domain has an important role in regulating this hydrolysis, the large

concerted motions centered on the active site, and consequently the GTP molecule, may be involved in this process.

The hypothesis that glycines 56 and 179 are critical for the motion between the two domains, which may in turn be necessary for the GDP/GTP exchange activity, will be tested by mutational experiments. These experiments are necessary, since there is no biochemical evidence, so far, showing the importance of these residues. The involvement of the switch I and II regions in GDP/GTP exchange is well studied. Lee et al. (1992) reported biochemical differences in $G\alpha_s$ when Gly 226 was mutated to alanine (Gly 199 in $G\alpha_t$). The mutant could bind GDP and GTP with same affinity as the native protein. However, the activated α subunit was unable to dissociate from $\beta\gamma$ subunits and consequently its ability to activate the effector was significantly reduced. The authors suggested that the conformational change, which occurs in the switch II region upon GDP/GTP exchange, was blocked by the mutation. This experiment also showed that although the switch II region is involved with ligand exchange, it does not affect the motion between the two domains, the subject of this paper, since the GDP release was not affected by the mutation.

Comparison of the dynamics of the GTPase domains of $G\alpha_t$ and *ras* p21 shows that these domains are not just structurally similar but also have similar large concerted motions in their common structural core. Although the two proteins catalyze much the same reaction and are homologous in structure, despite their low sequence identity, it does not necessarily follow that all their characteristics and mechanisms of action will be the same. The mechanism by which the rate of GTP hydrolysis in G-proteins is controlled is still the subject of debate. However, there are some relevant biochemical data in *ras* proteins, showing the importance of a set of key residues (Hilgenfeld, 1995; Schweins et al., 1994, 1995, 1996). Muegge et al. (1996) have determined the electrostatic contribution of individual residues to the binding of GDP and GTP to *ras* proteins, giving insights into the side chains involved in GTP hydrolysis. There is high conservation of these residues among the GTPase family. Thus, it is interesting to note that the dynamics simulations carried out here demonstrate similar binding modes and dynamics for two members of the family, which may reflect the effects of a few important residues common to them.

ACKNOWLEDGMENT

We thank Dr. Gert Vriend for helpful discussions during this work and Dr. Daniel Rigden for critically reading the manuscript and for his help in the center of mass calculations and preparing the stereo pictures.

REFERENCES

Ahmadian, M. R., Stege, P., Scheffzek, K. & Wittinghofer, A. (1997) *Nat. Struct. Biol. 4*, 686−689.
Amadei, A., Linssen, A. B. M., & Berendsen, H. J. C. (1993) *Proteins*: *Struct., Funct., Genet. 17*, 412−425.
Barbacid, M. (1987) *Annu. Rev. Biochem. 56*, 779−827.
Berman, D. M., Wilkie, T. M., & Gilman, A. G. (1996) *Cell 86*, 445−452.
Berstein, G., Blank, J. L., John, D. Y., Exton, J. H., Rhee, S. G., Ross, E. M. (1992) *Cell 70*, 411−418.
Diederichs, K., & Schulz, G. E. (1991) *J. Mol. Biol. 217*, 541−549.
Gibbs. J. B., Sigal, I. S., & Scolnick. E. M. (1985) *Trends Biochem. Sci. 10*, 350−353.
Graham, H. C., Williams, R. J. P., Littlechild, J. A., & Watson, H. C. (1991) *Eur. J. Biochem. 196*, 261−269.
Hilgenfeld, R. (1995) *Curr. Opin. Struct. Biol. 5*, 810−817.
Hunt, T. W., Fields, T. A., Casey, P. J., & Peralta, E. G. (1996) *Nature 383*, 175−177.
Kabsch, W., & Sander, C. (1983) *Biopolymers 22*, 2577−2637.
Kleus, C., Raw, A. S., Lee, E., Sprang, S. R., & Gilman, A. G. (1994) *Proc. Natl. Acad. Sci. U.S.A. 91*, 9828−9831.
Koelle, M. R. (1997) *Curr. Opin. Cell Biol. 9*, 143−147.
Lambright, D. G., Noel, J. P., & Sigler, P. B. (1994) *Nature 369*, 621−628.
Lambright, D. G., Sondek, J., Bohm, A., Skiba, N. P., Hamm, H. E., & Sigler, P. B. (1996) *Nature 379*, 311−319.
Lee, E., Taussig, R., & Gilman, A. G. (1992) *J. Biol. Chem. 267*, 1212−1218.
Markby, A. W., Onrust, R., & Bourne, H. R. (1993) *Science 262*, 1895−1901.
Marques, O., & Sanejouand, Y. H. (1995) *Proteins: Struct., Funct., Genet. 23*, 557−560.
Mello, L. V., van Aalten, D. M. F., & Findlay, J. B. C. (1997) *Protein Eng. 10*, 381−387.
Muegge, I., Schweins, T., Langen, R., & Warshel, A. (1996) *Structure 4*, 475−489.
Mueller, C. W., & Schulz, G. E. (1988) *J. Mol. Biol. 202*, 909−912.
Noel, J. P., Hamm, H. E., & Sigler, P. B. (1993) *Nature 366*, 654−663.
Pincus, M. R., Brandt-Rauf, P. W., Carty, R. P., Lubowsdy, J., Avitable, M., Gibson, K. D., Scheraga, H. A. (1987) *Proc. Natl. Acad. Sci. U. S. A. 84*, 8375−8379.
Schulz, G. E. (1991) *Curr. Opin. Struct. Biol. 1*, 883−888.
Schulz, G. E., Mueller, C. W., & Diederichs, K. (1990) *J. Mol. Biol. 213*, 627−630.
Schweins, T., Langen, R., & Warshel, A. (1994) *Nat. Struct. Biol. 1*, 476−484.
Schweins, T., Geyer, M., Scheffzek, K., Warshel, A., Kalbitzer, H. R., & Wittinghofer, A. (1995) *Nat. Struct. Biol. 2*, 36−44.
Schweins, T., Geyer, M., Kalbitzer, H. R., Wittinghofer, A., & Warshel, A., (1996) *Biochemistry 35*, 14225−14231.
Tesmer, J. J. G., Berman, D. M., Gilman, A. G., & Sprang, S. R. (1997) *Cell 89*, 251−261.
Tong, L. A., de Vos, A. M., Milburn, M. V., & Kim, S. H. (1991) *J. Mol. Biol. 217*, 503−516.
Van Aalten, D. M. F., Findlay, J. B. C., Amadei, A., & Berendsen, H. J. C. (1995a) *Protein Eng. 8*, 1129−1135.
Van Aalten, D. M. F., Amadei, A., Linssen, A. B. M., Eijsink, V. G. H., Vriend, G. & Berendsen, H. J. C. (1995b) *Proteins: Struct., Funct., Genet. 22*, 45−54.
Van Aalten, D. M. F., Jones, P. C., Sousa, M., & Findlay, J. B. C. (1997) *Protein Eng. 10*, 31−37.
Van Gunsteren, W. F., & Berendsen, H. J. C. (1987) *BIOMOS, Biomolecular Software*, Laboratory of Physical Chemistry, University of Groningen, Groningen, The Netherlands.
Vriend, G. (1990) *J. Mol. Graphics 8*, 52−56.
Watson, N., Linder, M. E., Druey, K. M., Kehrl, J. H., & Blumer, K. J. (1996) *Nature 383*, 172−175.

BI971402V